Large Molecule Therapeutics

Molecular Cancer Therapeutics

SGN–LIV1A: A Novel Antibody–Drug Conjugate Targeting LIV-1 for the Treatment of Metastatic Breast Cancer

Django Sussman, Leia M. Smith, Martha E. Anderson, Steve Duniho, Joshua H. Hunter, Heather Kostner, Jamie B. Miyamoto, Albina Nesterova, Lori Westendorf, Heather A. Van Epps, Nancy Whiting, and Dennis R. Benjamin

Abstract

In this article, we describe a novel antibody–drug conjugate (ADC; SGN–LIV1A), targeting the zinc transporter LIV-1 (SLC39A6) for the treatment of metastatic breast cancer. LIV-1 was previously known to be expressed by estrogen receptor–positive breast cancers. In this study, we show that LIV-1 expression is maintained after hormonal therapy in primary and metastatic sites and is also upregulated in triple-negative breast cancers. In addition to breast cancer, other indications showing LIV-1 expression include melanoma, prostate, ovarian, and uterine cancer. SGN–LIV1A consists of a humanized antibody conjugated through a proteolytically cleavable linker to monomethyl auristatin E, a potent microtubule-disrupting agent. When bound to surface-expressed LIV-1 on immortalized cell lines, this ADC is internalized and traffics to the lysozome. SGN–LIV1A displays specific *in vitro* cytotoxic activity against LIV-1–expressing cancer cells. *In vitro* results are recapitulated *in vivo* where antitumor activity is demonstrated in tumor models of breast and cervical cancer lineages. These results support the clinical evaluation of SGN–LIV1A as a novel therapeutic agent for patients with LIV-1–expressing cancer. *Mol Cancer Ther; 13(12); 2991–3000. ©2014 AACR.*

Introduction

In the United States, nearly 300,000 women are diagnosed with breast cancer each year and it is the second leading cause of cancer-related mortality in women. Surgery, radiation, hormone therapy, and chemotherapy are effective treatments for many, but over 40,000 patients succumb to the disease annually. Breast cancers are classified on the basis of three protein expression markers: estrogen receptor (ER), progesterone receptor (PgR), and the overexpression of the growth factor receptor HER2/neu. Hormonal therapies, including tamoxifen and aromatase inhibitors, can be effective in treating tumors that express the hormone receptors ER and PgR. HER2-directed therapies are useful for tumors that express HER2/neu; these tumors are the only class of breast cancer that is currently eligible for immunotherapy. For these patients, unconjugated antibodies (Herceptin, Perjeta) are generally used in combination with chemotherapy. The treatment options for triple-negative breast tumors, those that do not express ER, PgR, or HER2/neu, are restricted to chemotherapy, radiation, and surgery. In addition, there are limited effective treatment options available to patients with advanced-stage disease with relatively poor survival rates of stage III patients (52%) and significantly worse for stage IV patients (15%). There is clearly a significant need for effective treatments for late-stage breast cancer.

Antibody–drug conjugates (ADC) are a relatively new treatment modality that takes advantage of the exquisite specificity of monoclonal antibodies by using them to deliver a highly potent cytotoxic agent. The ADC described here is an anti–LIV-1 antibody linked via a cleavable dipeptide linker to monomethyl auristatin E (MMAE), the cytotoxic agent. Although there are at least 21 ADCs in clinical development (nine auristatin-based; ref. 1), only one is approved for use in breast cancer (Kadcyla for $HER2^+$ patient populations).

LIV-1 is a member of the solute carrier family 39; a multi-span transmembrane protein with putative zinc transporter and metalloproteinase activity (2, 3). It was first identified as an estrogen-induced gene in the breast cancer cell line ZR-75-1 (4). LIV-1 expression has been linked to epidermal-to-mesenchymal transition (EMT) in both normal vertebrate embryo development (5) and preclinical models (6–8) leading to malignant progression and metastasis. There is evidence of LIV-1 interacting with the transcription factors STAT3 and Snail to downregulate expression of E-cadherin to promote EMT (9, 10). Expression is also associated with lymph node involvement in breast cancer (11). In addition to

Seattle Genetics, Inc., Bothell, Washington.

Note: Supplementary data for this article are available at Molecular Cancer Therapeutics Online (http://mct.aacrjournals.org/).

Corresponding Author: Django Sussman, Seattle Genetics, Inc., 21823 30th Drive SE, Bothell, WA 98021. Phone: 425-527-4630; Fax: 425-527-4609; E-mail: dsussman@seagen.com

doi: 10.1158/1535-7163.MCT-13-0896

breast cancer, it has been detected in other neoplastic tissue types, including pancreatic, prostate, breast, melanoma, cervical, and uterine (8, 12, 13). We evaluated LIV-1 expression in a number of indications using immunohistochemical analysis on tissue biopsies. In addition, we performed quantitative flow cytometry to determine expression of LIV-1 on a panel of cell lines derived from various cancer types. Using a humanized antibody specific for LIV-1 (hLIV22) conjugated to MMAE (14), we demonstrated ADC internalization, *in vitro* cytotoxicity, and antitumor activity in *in vivo* breast and cervical cancer models.

Materials and Methods

Cell lines and culture

MCF-7 cells were obtained from three different sources: MCF-7 (ATCC HTB-22) from the American Type Culture Collection (ATCC), MCF-7 DSMZ from Deutsche Sammlung von Mikroorganismen und Zellkulturen (DSMZ), and MCF-7 NCI from NCI-Frederick Cancer Cell Line Repository (NCI-Frederick, MD). Other cell lines were obtained from the ATCC with the exception of PC-3 and HupT3 cells which were obtained from DSMZ. All cell lines were received before 2010 and cultured according to the supplier's recommendations; cell lines used for *in vitro* cytotoxicity (MCF-7 ATCC) and *in vivo* efficacy studies (MCF-7 NCI and HELA) were authenticated using the Cell Check service provided by IDEXX Bioresearch [identity confirmation by short tandem repeat (STR)–based DNA profiling and multiplex PCR]. A Chinese Hamster Ovary (CHO) cell line expressing human LIV-1 was generated by transfecting a CHO DG44 cell line with a plasmid coding for the intact LIV-1 gene. DHFR selection was used to identify positive clones.

Antibody humanization

The murine antibody mLIV22 specifically binds an epitope in the extracellular N-terminus (residues 1–329) of LIV-1. Complementarity-determining region (CDR) grafting was used to generate the humanized anti–LIV-1 antibody hLIV22. First, the mLIV22 VL CDRs [as defined by Kabat (15)] were grafted on to the framework regions of human germline exons IGKV2-30 and JK4 obtained from NCBI and fused to human kappa constant domain. Likewise, the CDRs of mLIV22 VH were grafted onto the framework regions of human germline exons VH1-2 and JH5 fused to the human IgG1 constant domains. In addition, framework mutations, F36Y and R46P in the light chain and Y27L, F29I, T30E, S76N, and R94V of the heavy chain (numbering scheme of Kabat), were introduced into the humanized variable domains to enhance antigen-binding activity. The resultant humanized anti–LIV-1 antibody, hLIV22, showed comparable antigen-binding activity to mLIV22 in competition-binding assays using CHO cells transfected with LIV-1.

Immunohistochemistry

Formalin-fixed paraffin-embedded (FFPE) tumor samples were obtained from several sources: the Cooperative Human Tissue Network, Tissue Solutions; National Disease Research Interchange (NDRI; Philadelphia, PA). Slides were deparaffinized and antigen retrieval was performed using EDTA-based buffer. Samples were preblocked with nonserum protein block (Dako A/S) and primary antibodies, used separately, were incubated for 45 minutes at room temperature. Anti–LIV-1 mAb and isotype control IgG were used at 1 μg/mL. Bond Polymer Refine Detection (Leica Microsystems) was used for detection with 3,3′-diaminobenzidine as the substrate for horseradish peroxidase (HRP) and Bond Polymer Refine Red Detection (Leica Microsystems) was used for detection with Fast Red as substrate for alkaline phosphatase. Slides were then scored using a qualitative scoring scale (weak 1+, mild 2+, moderate 3+, strong 4+) and images were taken using a Zeiss Axiovert 200 M microscope (Carl Zeiss Microimaging). For mouse xenograft tumors, biotinylated LIV-1 antibody and the Bond Intense R Detection Kit (Leica Microsystems, Germany) were used.

Quantitative flow cytometry

Cell surface LIV-1 expression levels were measured using QIFIKIT flow cytometric indirect immunofluorescence assay (Dako A/S) using mLIV-14 as the primary antibody. A total of 5×10^5 cells per sample were incubated with a saturating concentration (10 μg/mL) of primary antibody for 60 minutes at 4°C. After washes, FITC-conjugated secondary antibody (1:50 dilution) was added for 45 minutes at 4°C. Fluorescence was analyzed by flow cytometry and specific antigen density was calculated on the basis of a standard curve of log geometric mean fluorescence intensity versus log antigen-binding capacity.

Competition binding

LIV-1–expressing 293F cells (1×10^5) in PBS were aliquotted in each well of 96-well v-bottom plates on ice. The cells were incubated for 1 hour with 5 nmol/L Alexa Fluor 647–labeled hLIV22 and increasing concentrations (from 0.03 to 500 nmol/L) of unlabeled mLIV22, hLIV22, or SGN–LIV1A. Cells were pelleted and washed two times with PBS. The cells were then pelleted and resuspended in 125 μL of PBS/FBS. Fluorescence was analyzed by flow cytometry, using percentage of saturated fluorescent signal to determine percentage of labeled mLIV22 bound and to subsequently extrapolate the half-maximal inhibitory concentrations (IC_{50}) by fitting the data to a sigmoidal dose–response curve with variable slope.

Conjugation of antibodies

The hLIV22-vcMMAE ADC was prepared by partial reduction of antibody interchain disulfide bonds with tris (2-carboxyethyl)-phosphine (TCEP) followed by conjugation to maleimidocaproylvaline-citrulline-p-aminobenzyloxycarbonyl-MMAE (vcMMAE) as described previously

(16) with the following modifications. Partial reduction of the interchain disulfide bonds, to an average of two reduced disulfide bonds or four reactive thiols per antibody, was achieved by incubating antibody solutions with 2.5 mol/L equivalents of TCEP at 37°C in the presence of 1 mmol/L diethylenetriaminepentaacetic acid for 1.5 hours. Final drug loading was determined by reverse-phase high-performance liquid chromatography under reducing conditions and by hydrophobic interaction chromatography (16).

Fluorescence microscopy

ADC internalization images. MCF7 cells were plated on fibronectin-coated 8-well chamber slides (BD Biosciences) and allowed to grow for 2 days at 37°C in appropriate media. Cells were then incubated with 1 μg/mL SGN–LIV1A with or without 10 μmol/L chloroquine for 0, 4, or 24 hours at 37°C. Cells were fixed and permeabilized using Cytofix/Cytoperm solution (BD Biosciences). ADC was detected with goat anti-human IgG Alexa Fluor 488 (Invitrogen). LAMP1, a lysosomal marker, was detected with biotinylated mouse anti-human CD107a (BD Biosciences), followed by Alexa Fluor 594–conjugated streptavidin (Invitrogen). Cells were mounted in ProLong Gold Antifade with DAPI (Invitrogen). Images were acquired with a 63× oil objective on an Axiovert 200 M inverted fluorescence microscope. Microtubule Network Images. MCF7 cells were plated on D-lys–coated 8-well chamber slides (BD Biosciences) and allowed to grow for 2 days at 37°C in appropriate media. Cells were then incubated with 1 μg/mL or 10 ng/mL SGN-LIV1a for 0 or 24 hours at 37°C. Cells were fixed as described above. Tubulin was detected with mouse anti-α-tubulin Alexa Fluor 488 (Invitrogen). Cells were mounted in SlowFade with DAPI (Invitrogen). Images were acquired with a 63× oil objective on an Axiovert 200 M inverted fluorescence microscope.

Cytotoxicity assay

Tumor cells were incubated with SGN–LIV1A or hLIV22 for 96 hours at 37°C. Cell viability was measured by CellTiter-Glo (Promega Corporation) according to the manufacturer's instructions. Cells were incubated for 25 minutes at room temperature with the CellTiter-Glo reagents and luminescence was measured on a Fusion HT fluorescent plate reader (PerkinElmer). Results are reported as EC_{50}, the concentration of compound needed to yield a 50% reduction in viability compared with vehicle-treated cells (control = 100%).

PK methods

Six BALB/c mice were dosed i.v. with 3 mg/kg of SGN–LIV1A. Blood samples were drawn from the saphenous vein from alternating subgroups of 3 mice at 5 minutes, 6 and 24 hours, 2, 4, 7, 10, and 14 days after dose and processed to plasma. Samples were analyzed in a plate-based assay as follows: wells were coated overnight with a solution (0.5 μg/mL in 0.05 mol/L carb/bicarb buffer, pH 9.6) of anti-human IgG kappa antibody (Antibody solutions; #AS75-P). After washing with PBS-T, wells were blocked with 1% BSA for 1 hour at room temperature. After washing blocked plates with PBS-T, wells were incubated with samples at room temperature. After 1 hour, plates were washed with PBS-T and incubated for an additional hour with HRP-F(ab′)2 goat anti-human IgG Fc-gamma–specific (The Jackson Laboratory; #109-036-098). Following a final wash step, TMB substrate was added and incubated for 10 minutes before quenching with 1 N HCL, A_{450} was read and used to calculate serum antibody concentration

In vivo activity studies

Tumor volume was calculated using the formula, $(A \times B^2)/2$, where A and B are the largest and second largest perpendicular tumor dimensions, respectively. Mean tumor volume and weight of mice were monitored and mice terminated when the tumor volume reached 1,000 mm^3.

For MCF7-NCI and BR0555 studies, NOD.Cg-Prkdc^{scid} Il2rg^{tm1Wjl}/SzJ mice (NSG; The Jackson Laboratory) were implanted subcutaneously with 17β-estradiol 90-day time release tablets (Innovative Research of America). Animals were allowed 2 to 6 days recovery time from tablet implant before receiving cell or tissue implant. 17β-Estradiol tablets were implanted every 90 days thereafter.

MCF7-NCI cells were implanted at 5×10^6/200 μL Matrigel HC25% (BD Biosciences). Once tumors reached a mean tumor volume of 100 mm^3, mice were treated by intraperitoneal injection every 4 days for a total of four doses with either SGN–LIV1A (1 or 3 mg/kg) or human IgGvcMMAE (hIg-vcMMAE) as a nonbinding control. An additional group of tumor-bearing mice ($n = 5$) was left untreated as a control.

BR0555 is a subcutaneous model derived from a patient with primary breast cancer (The Jackson Laboratory). NSG mice bearing tumors between 500 and 750 mm^3 were sacrificed and the tumors were removed using aseptic technique. Tumors were sectioned into small fragments approximately 3 to 5 mm^3 and loaded into 14-gauge trocars. Mice were implanted subcutaneously in the right lateral flank and returned to a clean home box. Implanted mice were monitored once a week and started on study when their tumor reached approximately 250 mm^3. In this model, mice enrolled to the study in a patient accrual fashion; days 58 through 78, and dosing started. At each evaluation, the available cohort of mice was distributed to study groups in an equal fashion with an $n = 10$ per group. Mice were treated by intraperitoneal injection every 4 days for a total of four doses with either SGN–LIV1A (1 or 3 mg/kg) or hIg-vcMMAE as nonbinding control. An additional group of tumor-bearing mice was left untreated as a control.

In the HeLa (ATCC CLL-2) *in vivo* study, female Athymic Nude-*Foxn1*^{nu} (Harlan) were implanted with tissue

fragments of tumors maintained in serial passage. Tumors were sectioned into small fragments approximately 3 to 5 mm^3 and loaded into 14-gauge trocars. Mice were implanted subcutaneously in the right lateral flank and returned to a clean home box. On day 10 after implant, the mice were evaluated and randomly placed into study groups ($n = 8$) with a mean tumor size of approximately 100 mm^3 and dosing was started. Mice were treated by intraperitoneal injection every 4 days for a total of four doses with either SGN–LIV1A (1 or 3 mg/kg) or hIg-vcMMAE as nonbinding control. An additional group of tumor-bearing mice was left untreated as a control.

Results

LIV-1 is highly expressed in solid tumors of different origins

LIV-1 expression was evaluated in human normal tissue and tumor microarrays and in sets of larger tissue sections. LIV-1 is frequently expressed in breast, prostate, and melanoma, even in patients previously treated with hormonal therapies (Table 1 and Fig. 1). In contrast, ovarian, uterine, and lung cancers have measurable, but less frequent, LIV-1 expression. An extensive panel of normal human tissues were also examined and showed limited LIV-1 expression (Table 2 and Fig. 1). The normal tissues that stain positive for LIV-1 expression in IHC have variable expression. In breast tissue, 0% to 50% of the cells stain with an intensity of 1 to 2 on the same scale used for the neoplastic tissue. In prostate tissue, 50% to 100% of the cells stain with an intensity of 2 to 4. In testicular tissue, about 50% of the cells stain with an intensity up to 1. The broad expression of LIV-1 in breast, prostate, and melanoma tumors, coupled with the restricted normal tissue expression (breast, prostate, and testis), demonstrate that LIV-1 is a target well suited for an ADC therapeutic. The expression is most prominent in breast cancer, the focus of this study.

LIV-1 is highly expressed in post–hormone-treated primary and metastatic breast tumors

To determine the expression of LIV-1 in breast carcinomas, a murine anti–LIV-1 mAb was used for the detection in FFPE samples by IHC. We found that large sections of tumor samples provided better measure of LIV-1 expression in the tumor samples analyzed compared with commercially available tumor microarrays.

Because there is known positive correlation between LIV-1 expression and ER, we also evaluated breast tumor samples in which the patients had previously received hormone therapy for their ER^+ cancers. We analyzed expression in breast cancer biopsies in patients having received hormonal therapy (tamoxifen or aromatase inhibitors). A total of 82 post–hormone therapy biopsies were studied and 88% of these expressed LIV-1 (at any level of intensity or %positive). As illustrated in Fig. 1A, 92% of primary site post-hormone-treated tumor biopsies expressed LIV-1 with intensity of the staining ranging from weak (1–2+) to strong (3–4+). About 50% of the cases had $\geq$50% to 100% of tumor cells expressing LIV-1. Good concordance was observed with the reactivity of another anti–LIV-1 mAb in formalin-fixed tissues (data not shown). The immunostaining pattern was characterized as both membranous and cytoplasmic. The staining was LIV-1 specific, based on concordant reactivity between the two anti–LIV-1 mAbs used and the absence of staining with an isotype-matched negative control antibody. We also studied post–hormonal therapy metastatic breast tumor biopsies. Eighteen out of 23 cases (78%) expressed LIV-1, with approximately 75% of cases staining $\geq$50% to 100% of the tumor cells (Fig. 1B).

Expression of LIV-1 in triple-negative (ER^-, PgR^-, Her-2-unamplified) primary breast tumors was also evaluated. We observed 65% LIV-1^+ in a set of 20 cases, with 40% (8 of 20) showing $\geq$50% to 100% of tumor cells positive, albeit with lower intensity of LIV-1 expression (Fig. 1C) compared with ER^+ cases. Representative images of staining intensity are shown in Fig. 1D.

Quantitative flow cytometric analysis of LIV-1 expression on human cancer cell lines

Cell surface expression of LIV-1 in human tumor cell lines was evaluated using quantitative flow cytometry. The panel of cell lines included breast, cervical, head and neck, hepatocellular, kidney, ovarian,

Table 1. LIV-1 expression in multiple cancer types

Neoplastic tissue	Number of positive samples	Number of samples examined	% Positive
Breast	88	95	93
Melanoma	42	51	82
Prostate	36	50	72
Ovary	10	21	48
Uterus	6	20	30*
Lung	3	30	10*

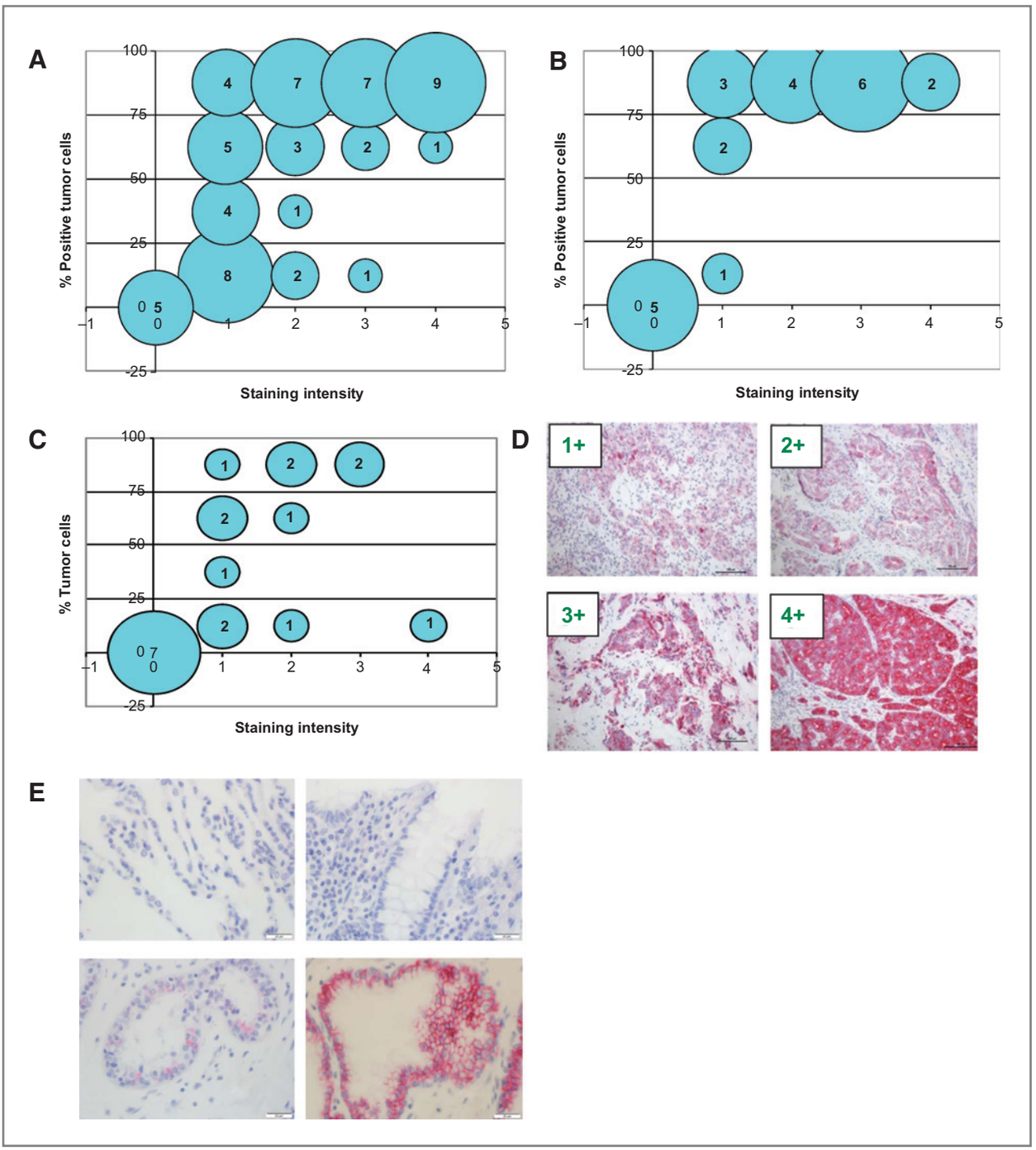

Figure 1. A–D, LIV-1 is expressed in primary and metastatic post–hormone-treated breast cancer cases. Tissue sections were preserved in formalin, expression was detected using Fast Red as a substrate for alkaline phosphatase. A, 54 of 59 (92%) of posttreatment, primary site breast cancer biopsies express LIV-1. B, 18 of 23 (78%) of posttreatment, metastatic breast cancer biopsies express LIV-1. C, 13 of 20 (65%) of primary site triple-negative breast cancer biopsies express LIV-1. D, examples of tissues with LIV-1–specific staining intensity of 1–4. E, examples of normal tissue staining, clockwise from top left: lung, colon, prostate, and breast.

pancreatic, prostate, and melanomas. The highest level of LIV-1 expression was observed in the MCF-7 breast cancer cell line from the ATCC (175,000 sites/cell) while ZR-75-1 (ATCC CRL-1500) had about 80,000 sites per cell (Table 3). Other cell lines (ovarian, pancreatic, head and neck, and melanomas) showed moderate to low level expression of LIV-1 by qFACS.

Table 2. LIV-1 expression in normal tissue

Normal tissues negative for anti–LIV-1 staining		
Adrenal gland	Kidney	Skin
Bone	Larynx	Spleen
Cerebellum and cerebrum	Liver	Stomach
Colon	Lung	Striated muscle
Esophagus	Mesothelium	Thymus gland
Eye	Ovary	Thyroid
Heart	Parathyroid gland	Tonsil
Hypophysis	Salivary gland	Uterine cervix
Intestine		
Normal tissues positive for anti–LIV-1 staining		
Breast	Testis	
Prostate		

Humanized LIV-22 affinity

Parental murine LIV22 (mLIV22) was humanized to hLIV22 using the CDR grafting method. To ensure that neither humanization nor conjugation minimal effects on binding to LIV-1, the binding affinity of mLIV22 was compared with hLIV22 and SGN–LIV1A in a competition binding assay. The IC_{50} determined for mLIV22, hLIV22, and SGN–LIV1A were 3.5, 4.6, and 5.6 nmol/L, respectively. These data suggest that humanization did not significantly impact the binding affinity of hLIV22 to LIV-1.

Anti–LIV-1 ADCs are potent inhibitors of cell proliferation of MCF-7 breast carcinoma cells

The humanized LIV-1 antibody (hLIV-22) was conjugated to the antitubulin drug, vcMMAE, on reduced cysteines usually involved in interchain disulfide bonds with a mean stoichiometry of four drugs/antibody (16). The resulting ADC, SGN–LIV1A, has a potent cytotoxic activity against MCF-7 cell line (ATCC) with an EC_{50} value of 6.3 ng/mL in a CellTiter-Glo (Promega) cytotoxicity assay (Fig. 2B). In contrast, neither unconjugated parental antibody (Fig. 2) nor an ADC control hIgG-vcMMAE showed substantial cytotoxic activity (EC_{50} > 10,000 ng/mL; data not shown). In this assay, maximum cytotoxicity was 70%. When comparing a MCF-7 cell lines from different sources, we found they had varying concentrations of antigen on the surface of their plasma membrane. We have shown that decreasing amounts of antigen displayed on the surface of the cell have an adverse effect on *in vitro* cytotoxicity (Supplementary Table S1) of SGN–LIV1A. Incomplete cell killing with SGN–LIV1A could be due to a heterogeneous low antigen expressing or quiescent, slowly dividing cell subpopulation.

SGN-LIVA engages the target, internalizes, and traffics to the lysosome

Subcellular localization of SGN–LIV1A in MCF-7 cells (a LIV-1–positive cell line) was examined by fluorescence microscopy at 0, 4, and 24 hours. SGN-LIV1A internalizes slowly over a 24-hour period (Fig. 3A, top). To better visualize SGN–LIV1A accumulation within lysosomes, cells were treated with 10 μmol/L chloroquine to block ADC degradation (Fig. 3A, bottom). Nonbinding control ADC showed minimal binding and internalization into MCF-7 cells, with or without chloroquine (data not shown). A control nonlysosomal ADC internalized, but did not converge on the lysosome with 10 μmol/L chloroquine treatment, suggesting the SGN–LIV1A lysosomal localization is not simply a collapse of intracellular vesicles (data not shown). In summary, SGN–LIV1A internalizes throughout a 24-hour treatment period and traffics to the lysosome in which proteolytic release of the cytotoxic payload occurs.

Disruption of microtubules

Treatment of LIV-1–expressing MCF-7 cells with SGN-LIV1A at doses as low as 10 ng/mL for 24 hours induced disruption of the microtubule network (Fig. 3B). At 24 hours, 49% ($N = 150$; Fig. 2) of cells treated with 1 μg/mL SGN-LIV1a or 16% ($N = 100$) of cells treated with 10 ng/mL SGN-LIV1a displayed condensed chromosomes and abnormal spindles. At 24 hours, 0% ($N = 300$) of cells treated with nonbinding control displayed this phenotype. These data are consistent with the proposed mechanism of action leading to mitotic arrest.

PK and *in vivo* ADC activity study using MCF-7, BR0555, and HeLa tumors

To measure the pharmacokinetic (PK) properties of SGN–LIV1A, a single 3 mg/kg dose was administered i.v. to BALB/C mice; blood samples were taken out to 14 days. The PK properties of the total antibody appear consistent with a two compartment model (Fig. 4A). The terminal half-life, calculated using nonlinear regression, is 6.8 days.

Table 3. Quantitative flow data showing LIV-1 expression on cell lines of various origins

Cell line name	Source	LIV-1 copy number
MCF-7 (ATCC)	Breast	175,000
ZR-75-1	Breast	91,000
DU-4475	Breast	50,000
BT-20	Breast	46,000
MDA-MB-157	Breast	45,000
MDA-MB-175-VII	Breast	39,000
BT483	Breast	36,000
MDA-MB-231	Breast	32,000
T47D	Breast	25,000
MCF-7 (nci)	Breast	22,000
HeLa	Cervical	78,000
Detroit 562	Head and Neck	22,000
Hep3B	Hepatocellular	32,000
HEK293F	Kidney	59,000
SKOV3	Ovarian	71,000
ES-2	Ovarian	38,000
OVCAR-3	Ovarian	34,000
HupT3	Pancreatic	27,000
PC-3	Prostate	35,000
LNCAP	Prostate	32,000
22RV-1	Prostate	23,000
SKMEL-5	Melanoma	29,000
G361	Melanoma	25,000
A2058	Melanoma	16,000
WM115	Melanoma	12,000
Hs695T	Melanoma	22,000
Sk-Mel-2	Melanoma	19,000
MALME-3M	Melanoma	15,000
Skmel3	Melanoma	24,000
CHL1	Melanoma	16,000
HNCB	Melanoma	6,000

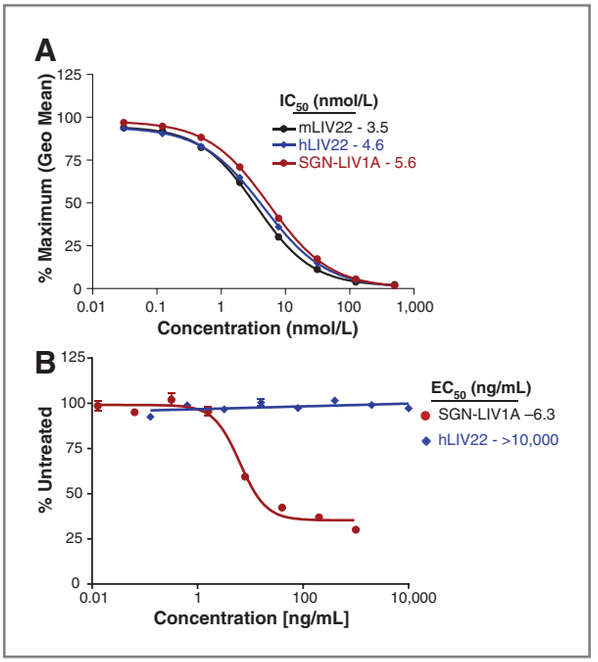

Figure 2. A and B, hLIV-22 retains binding affinity and has potent *in vitro* cytotoxicity activity as a conjugate. A, FACS-based competition binding experiments, performed by titrating unlabeled test article into cells with a constant concentration of labeled mLIV22 present, showed no post-humanization loss of affinity. B, MCF-7 ATCC cells were grown in 96-well plates, SGN–LIV1A or naked hLIV-22 were added for 96 hours before monitoring viability using CellTiter-Glo.

The antitumor activity of SGN–LIV1A was evaluated in xenograft models of breast, and cervical lineage. Two different breast cancer models were explored, one using MCF-7 cells and the other using a patient-derived tissue model. In the MCF-7 breast cancer cell xenograft model, tumor regressions were achieved with four 3 mg/kg doses of SGN–LIV1A given every 4 days (Fig. 4B), well below the mean-tolerated dose of 10 mg/kg in rodents. Although tumor growth delay was seen when dosing with the nontargeted ADC, when comparing it with the 3 mg/kg SGN–LIV1A dose group, P values compute to <0.05, meeting the threshold of statistical significance difference and indicating both a dose response and immunologic specificity of the targeted therapeutic. ADC activity in the absence of target has been documented previously on a number of antibody backbones and chemotype combinations (17–19). Noncancer antigen-dependent activity is a continuing topic of study and has been attributed to a combination of factors, including the enhanced permeability and retention effect of a tumor, ADC and drug linker stability, cellular susceptibility to the delivered cytotoxin, and relative cell permeability of the released drug.

The second breast cancer model (BR0555) was derived from the ER^+, PR^+, and HER2-infiltrating breast ductal carcinoma tumor from an 86-year-old Caucasian patient before any therapeutic intervention. Treatment of BR0555 tumor-bearing mice with SGN–LIV1A on a every 4 days schedule showed antitumor activity, resulting in pronounced tumor regressions (Fig. 4C).

SGN–LIV1A activity was also examined in the HeLa (cervical cancer–derived) xenograft model. Treatment with four 3 mg/kg doses of SGN–LIV1A given every 4 days resulted in significant tumor shrinkage compared with a nonbinding control ADC (Fig. 4D).

Discussion

ADCs directed toward tumor-specific antigens are clinically proven as effective treatments of both solid and liquid tumors. We have shown in this study that LIV-1, an integral cell surface membrane protein, is a promising candidate for ADC therapy due to its broad expression in a number of cancer indications and limited normal tissue expression. LIV-1 is expressed across an array of cell lines from various lineages with surface copy numbers ranging

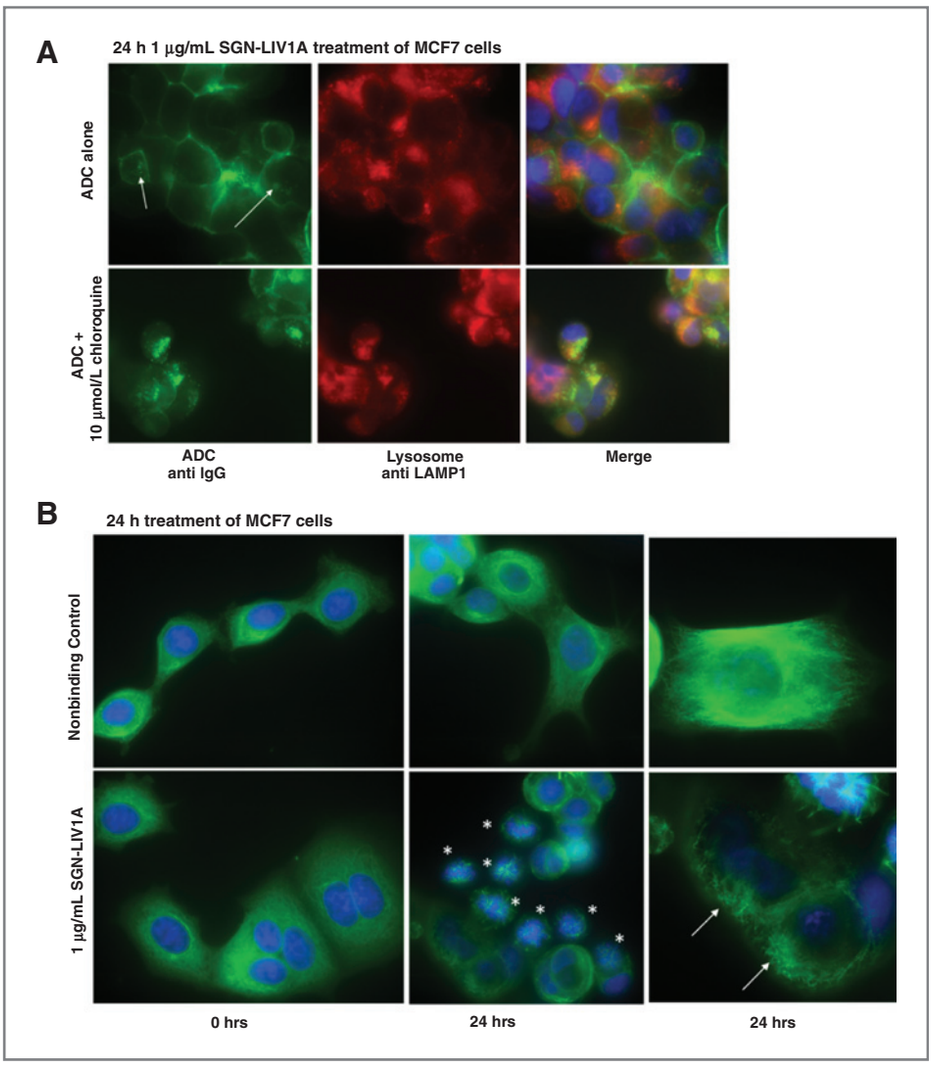

Figure 3. A and B, SGN–LIV1A internalizes, traffics to the lysosome, and disrupts the microtubule network in LIV-1–expressing cells. A, top, SGN–LIV1A–treated cells, arrows point to internalized ADC. Bottom, SGN–LIV1A + chloroquine–treated cells. ADC is stained green; LAMP 1, a lysosome-associated protein, is stained red; areas of colocalization show as orange. B, top, cells are incubated with nonbinding control ADC for 0 and 24 hours. Bottom, cells are incubated with SGN–LIV1A for 0 and 24 hours. Microtubules are stained green and DNA is stained blue.

from >170,000 to >5,000. Furthermore, inspection of archived biopsies showed a high percentage of primary, metastatic, and triple-negative breast cancer tissues that expressed the antigen. On the basis of these encouraging findings, we engineered a humanized anti–LIV-1 antibody that binds specifically to the extracellular domain of LIV-1, internalizes after antigen binding, and traffics to the lysosome. Using this antibody, we designed and generated SGN–LIV1A that leverages the specificity of the antibody and the activity of a potent microtubule-disrupting agent (MMAE) to produce a LIV-1–directed cytotoxic agent. SGN–LIV1A shows *in vitro* and *in vivo* potency and specificity when treating LIV-1–expressing cell lines and tumors.

In vitro assays showed that high LIV-1–expressing cell line was insensitive to treatment with the naked antibody alone. Cell lines that have low LIV-1 cell surface copy number are resistant to SGN–LIV1A and only show growth inhibition at concentrations >1,000 ng/mL.

We have shown that SGN–LIV1A is effective in *in vivo* xenograft models of different origin, including models of breast, prostate, and cervical lineage, delaying tumor growth at a relatively low dose (1 mg/kg/dose). Consistent with the proposed mechanism of ADC action, SGN–LIV1A was most effective *in vivo* on xenograft models with the highest expression of LIV-1, showing pronounced tumor regressions at doses of 3 mg/kg, while the antibody alone did not inhibit tumor growth at doses as high as 30 mg/kg. Cell surface LIV-1 copy number is difficult to accurately ascertain for tissues. However, IHC staining of xenograft sections indicates homogenous LIV-1 levels (100% of the cells) at an intensity of 2 to 3, which is equivalent or less than the staining seen in over 50% of the metastatic breast biopsy sections.

Dependent upon the tumor receptor expression profile, there are now several targeted therapeutic approaches that can be used, including HER2 and hormone-directed regimens. However, regardless of their classification, patients who have relapsed with distant-stage metastatic

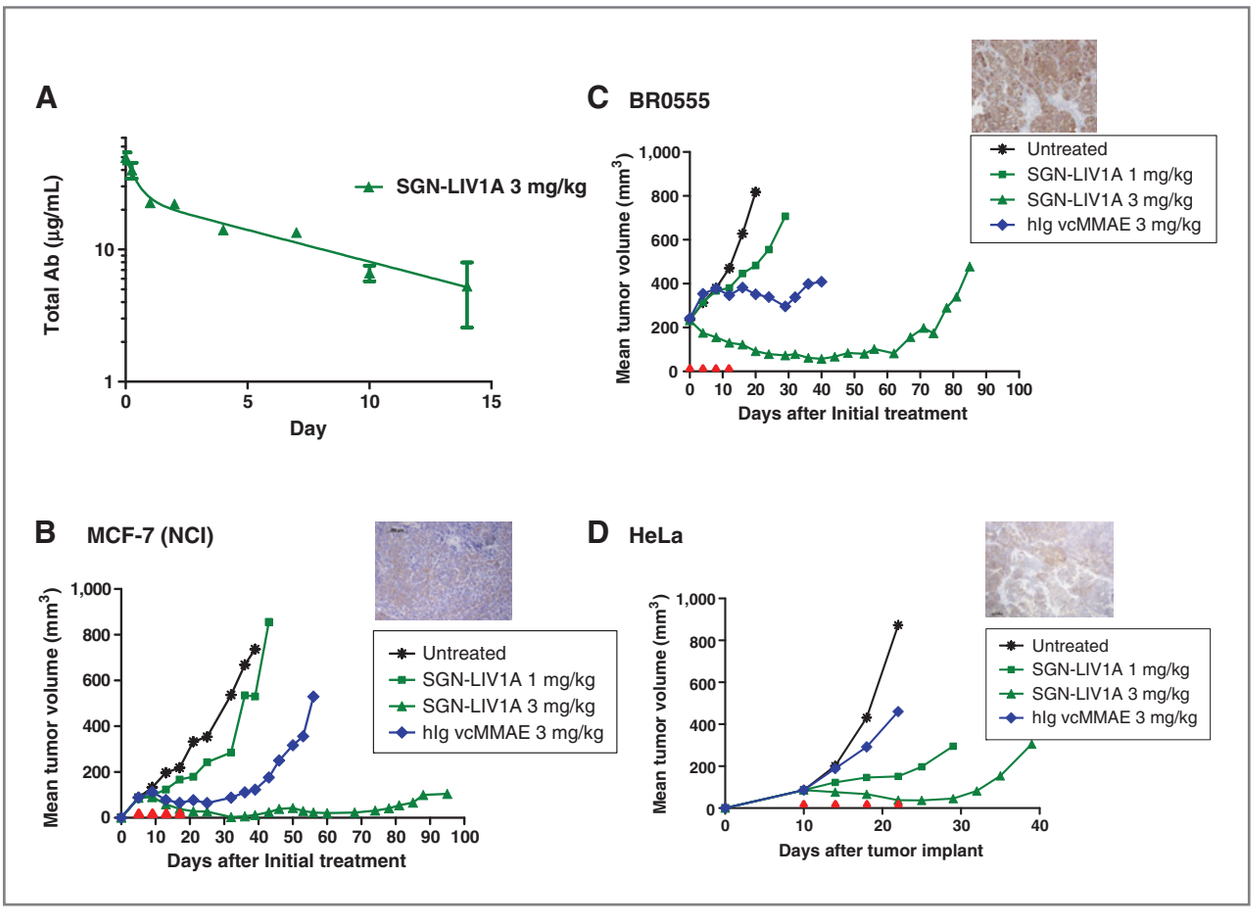

Figure 4. A–D, PK and *in vivo* model activity of SGN–LIV1A. A, top, the PK properties of the total antibody appear to follow a two compartment model. Bottom, the terminal half-life, calculated using nonlinear regression, is 6.8 days. B, NSG mice were implanted s.c. with MCF-7 NCI cells. Once tumors reached 100 mm^3, animals were treated with indicated doses of SGN–LIV1A or a nonbinding control every 4 days, a total of four times. C, NSG mice were implanted with fragments of BR0555 tumors, and once tumors reached 250 mm^3 they were treated as in B. D, nude mice were implanted with HeLa cells and treated as in B.

breast cancer have no curative therapeutic options open and face a 5-year survival rate of 24% (20). Current systemic treatments of these patients aim to prolong survival, control disease progression, alleviate symptoms, and enhance patient quality of life. In this study, we have shown that LIV-1 is expressed in all subtypes of breast cancer (including triple-negative) and that SGN–LIV1A is active as a single agent in preclinical models. These data in combination with the recent successes of ADCs support pursuing SGN–LIV1A as a new therapeutic modality for refractory metastatic breast cancer and other LIV-1–positive indications.

Disclosure of Potential Conflicts of Interest

D. Sussman, L.M. Smith, J.B. Miyamoto, A. Nesterova, L. Westendorf, and D.R. Benjamin have ownership interest (including patents) in Seattle Genetics, Inc. No potential conflicts of interest were disclosed by the other authors.

Authors' Contributions

Conception and design: D. Sussman, L.M. Smith, H.A. Van Epps, N. Whiting, D.R. Benjamin

Development of methodology: D. Sussman, L.M. Smith, J.H. Hunter, N. Whiting

Acquisition of data (provided animals, acquired and managed patients, provided facilities, etc.): L.M. Smith, M.E. Anderson, S. Duniho, H. Kostner, J.B. Miyamoto, A. Nesterova, L. Westendorf, H.A. Van Epps

Analysis and interpretation of data (e.g., statistical analysis, biostatistics, computational analysis): D. Sussman, L.M. Smith, S. Duniho, H. Kostner, J.B. Miyamoto, A. Nesterova, L. Westendorf, H.A. Van Epps, N. Whiting, D.R. Benjamin

Writing, review, and/or revision of the manuscript: D. Sussman, L.M. Smith, M.E. Anderson, S. Duniho, J.H. Hunter, J.B. Miyamoto, A. Nesterova, L. Westendorf, H.A. Van Epps, N. Whiting, D.R. Benjamin

Administrative, technical, or material support (i.e., reporting or organizing data, constructing databases): L.M. Smith

Study supervision: D. Sussman, L.M. Smith

Other (preparation of reagents): J.H. Hunter

Acknowledgments

The authors thank Jonathan Drachman for his careful review and assistance in completing this article.

The costs of publication of this article were defrayed in part by the payment of page charges. This article must therefore be hereby marked *advertisement* in accordance with 18 U.S.C. Section 1734 solely to indicate this fact.

Received October 21, 2013; revised August 20, 2014; accepted September 14, 2014; published OnlineFirst September 24, 2014.

References

1. Sievers EL, Senter PD. Antibody–drug conjugates in cancer therapy. Annu Rev Med 2013;64:15–29.
2. Taylor KM, Morgan HE, Johnson A, Hadley LJ, Nicholson RI. Structure-function analysis of LIV-1, the breast cancer-associated protein that belongs to a new subfamily of zinc transporters. Biochem J 2003;375:51–9.
3. Lopez V, Kelleher SL. Zip6-attenuation promotes epithelial-to-mesenchymal transition in ductal breast tumor (T47D) cells. Exp Cell Res 2010;316:366–75.
4. Manning DL, Daly RJ, Lord PG, Kelly KF, Green CD. Effects of oestrogen on the expression of a 4.4 kb mRNA in the ZR-75-1 human breast cancer cell line. Mol Cell Endocrinol 1988;59:205–12.
5. Yamashita S, Miyagi C, Fukada T, Kagara N, Che YS, Hirano T. Zinc transporter LIVI controls epithelial–mesenchymal transition in zebrafish gastrula organizer. Nature 2004;429:298–302.
6. Lue HW, Yang X, Wang R, Qian W, Xu RZ, Lyles R, et al. LIV-1 promotes prostate cancer epithelial-to-mesenchymal transition and metastasis through HB-EGF shedding and EGFR-mediated ERK signaling. PLoS ONE 2011;6:e27720.
7. Zhao L, Chen W, Taylor KM, Cai B, Li X. LIV-1 suppression inhibits HeLa cell invasion by targeting ERK1/2-Snail/Slug pathway. Biochem Biophys Res Commun 2007;363:82–8.
8. Unno J, Satoh K, Hirota M, Kanno A, Hamada S, Ito H, et al. LIV-1 enhances the aggressive phenotype through the induction of epithelial to mesenchymal transition in human pancreatic carcinoma cells. Int J Oncol 2009;35:813–21.
9. Taylor KM, Hiscox S, Nicholson RI. Zinc transporter LIV-1: a link between cellular development and cancer progression. Trends Endocrinol Metab 2004;15:461–3.
10. Huber MA, Kraut N, Beug H. Molecular requirements for epithelial–mesenchymal transition during tumor progression. Curr Opin Cell Biol 2005;17:548–58.
11. Manning DL, Robertson JF, Ellis IO, Elston CW, McClelland RA, Gee JM, et al. Oestrogen-regulated genes in breast cancer: association of pLIV1 with lymph node involvement. Eur J Cancer 1994;30A:675–8.
12. Dressman MA, Walz TM, Lavedan C, Barnes L, Buchholtz S, Kwon I, et al. Genes that co-cluster with estrogen receptor alpha in microarray analysis of breast biopsies. Pharmacogenomics J 2001;1:135–41.
13. Tozlu S, Girault I, Vacher S, Vendrell J, Andrieu C, Spyratos F, et al. Identification of novel genes that co-cluster with estrogen receptor alpha in breast tumor biopsy specimens, using a large-scale real-time reverse transcription-PCR approach. Endocr Relat Cancer 2006;13:1109–20.
14. Doronina SO, Toki BE, Torgov MY, Mendelsohn BA, Cerveny CG, Chace DF, et al. Development of potent monoclonal antibody auristatin conjugates for cancer therapy. Nat Biotechnol 2003;21:778–84.
15. Kabat EANational Institutes of Health (U.S.). Sequences of proteins of immunological interest. 5th ed. Bethesda, MD. Washington, DC: U.S. Dept. of Health and Human Services, Public Health Service For sale by U.S. G.P.O.; 1991.
16. Lyon RP, Meyer DL, Setter JR, Senter PD. Conjugation of anticancer drugs through endogenous monoclonal antibody cysteine residues. Methods Enzymol 2012;502:123–38.
17. Sharman JP, Oki Y, Advani RH, Bello CM, Winter JN, Yang Y, et al. A phase 2 study of brentuximab vedotin in patients with relapsed or refractory CD30-positive non-Hodgkin lymphomas: interim results in patients with DLBCL and other B-cell lymphomas, 2013. Presented at the 55th Annual Meeting and Exposition of the American Society of Hematology; December 7–10. 2013; New Orleans, LA.
18. Boghaert ER, Khandke K, Sridharan L, Armellino D, Dougher M, Dijoseph JF, et al. Tumoricidal effect of calicheamicin immunoconjugates using a passive targeting strategy. Int J Oncol 2006;28:675–84.
19. Kovtun YV, Audette CA, Ye Y, Xie H, Ruberti MF, Phinney SJ, et al. Antibody–drug conjugates designed to eradicate tumors with homogeneous and heterogeneous expression of the target antigen. Cancer Res 2006;66:3214–21.
20. Howlader N, Noone A, Krapcho M, Garshell J, Neyman N, Altekruse S, et al. SEER cancer statistics review, 1975–2010. Bethesda, MD: National Cancer Institute; 2013.